International Journal of
INTELLIGENT SYSTEMS AND APPLICATIONS IN ENGINEERING
ISSN:2147-6799 www.ijisae.org Original Research Paper

Mitigation of Ionospheric Scintillations Effect on NavIC Signals Using Multipath Parameter and Rate of TEC Index

G. Chandra Shekar*[1], P. Naveen Kumar[2]

Submitted: 07/05/2024 **Revised**: 20/06/2024 **Accepted**: 27/06/2024

Abstract: Improving the precision of Navigation with Indian Constellation (NavIC) positioning requires addressing the disturbances presented by ionosphere scintillation. Errors like cycle slip and measurement disparities are introduced by this phenomenon, which affects satellite lock and, in severe situations results in positioning failures. The usefulness of traditional scintillation parameters, S4 and σ_φ , is limited since they need high-frequency data. Using 1 Hz data, this research investigates the usage of the multipath parameter (MP) and the rate of total electron content index (ROTI) as substitutes for scintillation parameters. Satellite removal is greatly outperformed by procedures incorporating observation removal and noise matrix weighting, according to comparative analysis and validation against standard parameters (S4 and σ_φ). The suggested methods show an impressive 93.14% increase in Precise Point Positioning (PPP) outputs, proving that ROTI and MP are effective at reducing scintillation effects.

Keywords: *NavIC; Scintillation; Rate of TEC Index; Multipath parameter (MP); Precise Point Positioning*

1. Introduction

A common problem with the Global Navigation Satellite System (GNSS) is scintillation, which can cause problems including measurement inaccuracies, cycle slip, and signal loss. Its effects are most noticeable during geomagnetic storms, when it can lead to tracking error and even total signal loss [1],[2]. More than 70% of cycle slips have been shown to be significantly caused by strong scintillation, which also affects the phase lock loop (PLL) and lowers baseband signal power, further detuning the PLL frequency [3],[4]. This occurrence might result in fewer satellites accessible for tracking, which would constitute a serious threat to location. Numerous techniques have been put out to reduce the impact of scintillation on GNSS location, but many of them depend on scintillation parameters like S4 and σ_φ , which, in turn, describe the amplitude and phase of scintillation, respectively [5]. Furthermore, to improve the robustness of precise point positioning (PPP), receiver autonomous integrity monitoring (RAIM) has been utilised to identify and exclude scintillation-affected satellites [12]. Notwithstanding these attempts, difficulties still exist. Specifically, when utilising a single satellite constellation, signal lock loss and cycle slip continue to be the key problems under scintillation circumstances. In order to overcome these difficulties and provide location solutions that are more dependable in the presence of moderate to heavy scintillation, the integration of GPS and GLONASS data has been suggested [13].

In order to mitigate the impacts of scintillation on PPP, this work introduces two new strategies: the rate of change of the total electron content index (ROTI) and the multipath parameter (MP). Three ways of mitigation are suggested: (1) taking out the data from the most scintillation-affected satellite; (2) deleting the observations that are influenced by scintillation; and (3) weighting the measurement noise matrix in the Kalman Filter (KF) procedure. The performance of observation elimination and weighting procedures is evaluated against standard parameters (S4 and σ_φ), showing a significant increase in PPP outputs of up to 93.1%. It is discovered that in the suggested techniques, the performance of scintillation parameters and standard parameters is similar. Additionally, the study makes use of 1Hz data to improve scintillation studies. This makes it possible to study previous scintillation occurrences in more detail by using stored data. Using the higher frequency data available for more in-depth investigations, the ROTI is investigated as a stand-in for scintillation parameters [15–18]. In this study offers important new understandings on how to deal with the problems caused by ionosphere scintillation on NavIC signals. Promising results are seen when using the suggested solutions, which include multipath parameter (MP) and ROTI, to mitigate scintillation effects on precise point placement (PPP). The study highlights how important it is to use alternative parameters to improve our comprehension and mitigation techniques for scintillation of NavIC.

[1]*Research Scholar, Department of Electronics and Communication Engineering, University College of Engineering, Osmania University, Hyderabad-500 007, India.*
[2]*Professor, Department of Electronics and Communication Engineering, University College of Engineering, Osmania University, Hyderabad-500 007, India.*

** Corresponding Author Email: chandu.vnr2016@gmail.com*

2. Data and Methodology

2.1. Instrumentation and Data

Two different stations HYD (17.24^{0}N, 78.31^{0}E), KNL(15.79^0 N, 78.07^{0}E) data for a total of 70 days were used while stations use Accord IRNSS/GPS/SBAS receiver station. Data from 10 days were chosen for the PPP improvement tests, namely 7 and 3 days from the HYD and KNL stations, respectively. The techniques described in Li et al. [27] were used to identify scintillation events. Examples of the 10 days that were chosen include the following: November 7-13, 2017 (from HYD station); September 1-3 (KNL station). Also, the scintillation free data set were collected on September 1, 2017.

From the data, the multipath parameter (MP) and rate of change of the total electron content index (ROTI) were determined respectively. Also, from data scintillation parameters S4 and were produced at 1-minute intervals.

The mild threshold (MT) and extreme threshold (ET) were created using the full 70 days of data in order to identify outliers for the observation elimination technique. Li et al. [27] provide a comprehensive explanation of the methods used to determine MT and ET. In a nutshell, MT and ET are defined as follows:

$$MT=Q3+1.5IQR \quad (1)$$

$$ET=Q3+3IQR \quad (2)$$

$$\text{Where, } IQR=Q3-Q1 \quad (3)$$

Here, Q3 and Q1 represent the upper (3) and lower (1) quartiles, respectively, for height or 3D positioning errors. MT is the mild threshold, and ET is the extreme threshold. These thresholds are crucial for defining outliers in the observation removal strategy.

2.2. Rate of TEC Index

Pi et al. [29] first established the Rate of Change of Total Electron Content Index (ROTI) to evaluate scintillation events in the ionosphere. As per Pi et al.'s original definition [29], ROTI is calculated at a sample rate of 1 Hz with a 5-minute time interval. During ROTI computations, a moving average is used to guarantee temporal consistency with other metrics.

2.3. Multipath Parameters

Reflected signals can cause multipath interference, which affects GNSS receivers. According to Estey and Meertens [30], MP1 and MP2 are parameters that are used to measure the multipath impact.

2.4. Kalman Filter

The core method used in GNSS location to improve accuracy through the integration of many data is called the Kalman Filter (KF). The two main steps in the KF process are prediction and update. Every measurement is repeated in these processes [32]. A flowchart illustrating the sequential application of the Kalman Filter is shown in Figure 1.

In Figure 1, the covariance matrix is used as an estimate of state error, and the state and covariance matrix are built up during the initialization phase. Next, the process noise and dynamic model are added, which makes it easier to forecast the state and covariance matrices using either the initialised values or the updated values from the previous epoch. The variance between the input values and values generated from the preceding epoch is then used to construct the innovation vector.

Next, the value of the Kalman gain, which is essential for accounting for measurement error is found. The state and covariance matrix are updated by using the Kalman gain as the innovation vector's weighting factor. Predicting the state and covariance matrix for next iterations, this iterative process keeps on until all data are successfully processed. Full explanations of the Kalman Filter technique are included in the electronic supplement.

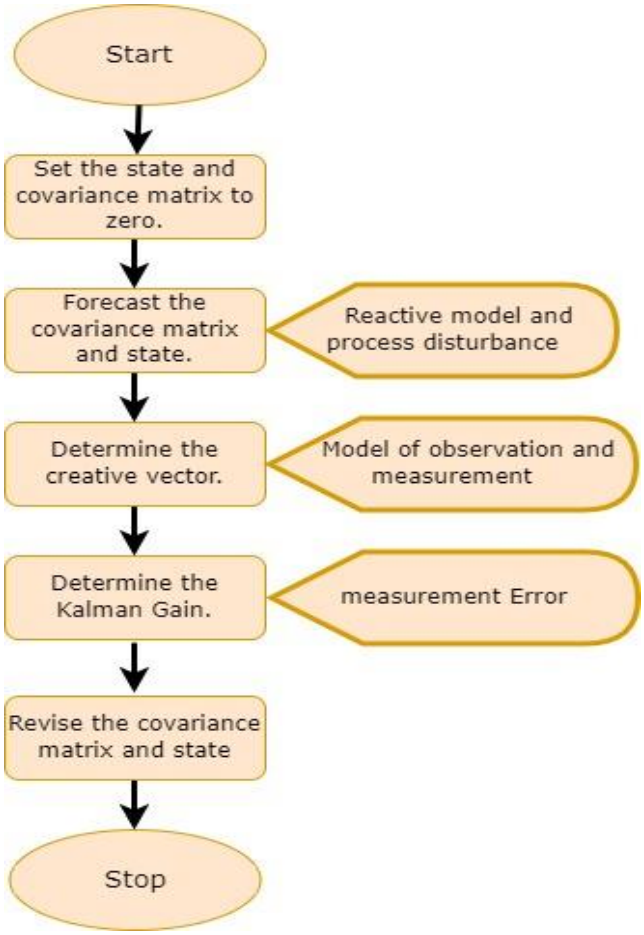

Figure 1: Kalman Filter Process Flowchart

2.5. Methodology

In accordance with the methodology described by An et al. [33], a day free of scintillation was selected for the assessment in order to determine the convergence time of PPPH. The convergence was calculated [33] and is defined as the point at which positioning accuracy achieves a certain tolerance (0.12m for the Up component). The methodical flowchart for reducing scintillation effects is shown in Figure 2. The initial data input was 10degree elevation mask scintillation day data, found using Li et al.'s methods [27]. To assess parameter efficacy, the first technique comprised removing the satellite with the greatest value iteratively five times for each reference parameter (MP1, MP2, ROTI, S4, and σ_φ). Interestingly, S4 was left out of satellite and observation removal procedures for the HYD station because of low S4 values at high latitudes [34].

Height and three-dimensional time series outputs were obtained by feeding both the original and processed data into PPPH. These results made it easier to calculate RMSE and associated improvement rates for processed and original data during scintillation-affected times. If scintillation happened early in the day, post-convergence RMSE computations were carried out. Furthermore, using the location of every visible satellite in relation to the receiver, Geometric Dilution of Precision (GDOP) was calculated to examine changes in the position and clock quality of satellites following removal. A portion of the design matrix was used to start the GDOP computations [36].

$$G = \begin{bmatrix} (x_0 - x^1)/p_0^1 & (y_0 - y^1)/p_0^1 & (z_0 - z^1)/p_0^1 & c \\ \vdots & \vdots & \vdots & \vdots \\ (x_0 - x^g)/p_0^g & (y_0 - y^g)/p_0^g & (z_0 - z^g)/p_0^g & c \end{bmatrix} \quad (4)$$

The GDOP calculation involved extracting the trace of the covariance matrix (cov(G)) to quantify the overall precision information encapsulated within G. This provided insights into the collective impact on the precision of position and clock estimates for the visible satellites.

$$GDOP = \sqrt{\sigma_x^2 + \sigma_y^2 + \sigma_z^2 + \sigma_t^2} = \sqrt{trace((G^T G)^{-1})} \quad (5)$$

Dilutions of Precision (DOP) values, more especially the Geometric Dilution of Precision (GDOP), are frequently used to evaluate the correctness of the geometric quality. According to the study [37], the GDOP computation entails calculating the root of the sum of the squares of the Root Mean Square Errors (RMSEs) for the clock (st) and estimated receiver coordinates (σ_x, σ_y, and σ_z). This computation is aided by the trace of the covariance matrix (cov(G)) which provides an overall measure of accuracy information.

In this case, lower DOP values are obtained, indicating more precision, when the satellites are positioned strategically, producing a stronger geometry. In general, DOP values of less than 5 and 10, respectively, are regarded as trustworthy for position and clock quality. To make it easier to see differences in lower GDOP values, GDOP values higher than 30 in this study were restricted at 30 [37].

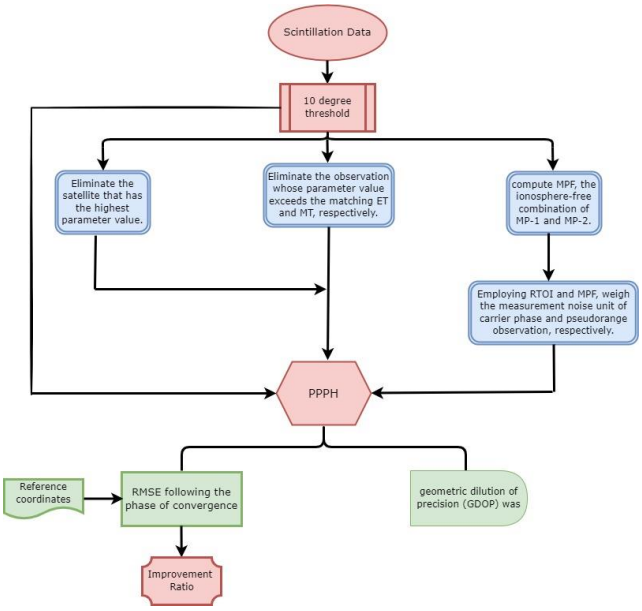

Figure 2. The three procedures are as follows: (1) weighing the observations, (2) removing satellites, and (3) observation removal.

In order to identify outliers for the second technique, parameter values have to exceed predetermined criteria. The Extreme Threshold (ET) and the Mild Threshold (MT) were the two threshold types that were compared in the study. In order to guarantee a thorough examination of data impacted by scintillation, several parameter combinations and permutations were investigated to get the best results. For comparison, standard parameters (MP and ROTI) and scintillation parameters (S4 and σ_φ) were taken into separate consideration.

For example, three combinations were investigated while taking scintillation characteristics into account: (1) S4; (2) σ_φ; and (3) S4 and σ_φ. Since S4 and σ_φ could contain outliers that S4 does not, it was hoped that combining the two will include more outliers and perhaps produce more accurate findings. Seven permutations were investigated in a similar manner for standard parameters. Crucially, this strategy was not replicated in satellite removal plans to minimize the possibility of the location algorithm failing entirely as a consequence of too much satellite removal, leaving less than four monitored satellites. After entering into PPPH, the identical processes used for the removal of satellites were repeated for the strategy of removal of observations.

As suggested by Mohammed [38], the third technique included an extra step that required computing the Ionosphere-Free (IF) combination of MP1 and MP2 (MPF). The multipath impact was down-weighted by using MPF. Even though IF combination reduced the major ionosphere error in MPF, scintillation-induced cycle lapses and the associated IF ambiguity may still have an effect on MPF. Given that carrier phase observations are more susceptible to scintillation [39], it was assumed as was the case with Roberts [40] that scintillation may have an impact on either carrier phase or pseudo range data. Given that multipath largely affects pseudo range data, MPF was mostly used to describe multipath while ROTI was used to describe ionosphere activity.

Using ROTI to weight the IF combination of carrier phase observation and MPF to weight the IF combination of pseudo range observation, the PPP method achieved the best improvement when compared to other weighting procedures.

Moreover, carrier phase and pseudo range observations were weighted using S4 and σ_{φ}, respectively. As is derived from signal carrier phase and S4 is computed from signal intensity, they serve as the corresponding effect factors for pseudo range and carrier phase. The measurement error covariance matrix R, which was presented in [32], was a prerequisite for the observation weights in the Kalman Filter (KF). Given that 'n' represents the total number of pseudo range and carrier phase observations, R might be initialized using the following formula, which expresses a 2n-by-2n identity matrix:

$$R = \begin{bmatrix} 1 & & \\ & \ddots & \\ & & 1 \end{bmatrix}_{2nx2n} \quad (6)$$

The original weight was then applied by multiplying it by each value along the diagonal of R, which was derived from the a priori standard deviation (SD) of measurements [32]:

$$R = \begin{bmatrix} P_{w,0} & & & & \\ & L_{w,0} & & & \\ & & \ddots & & \\ & & & P_{w,0} & \\ & & & & L_{w,0} \end{bmatrix}_{2nX2n} \quad (7)$$

$$P_{w,0} = SD_{0,P}^2 \left(\frac{f_1^2}{f_1^2 - f_2^2}\right)^2 \quad (8)$$

$$L_{w,0} = SD_{0,L}^2 \left(\frac{f_1^2}{f_1^2 - f_2^2}\right)^2 \quad (9)$$

The a priori standard deviations for code and phase measurements are thus represented by SD0P and SD0L, which are typically set at 3 m and 0.03 m, respectively [32, 41]. Next, the starting weights for the code and phase measurements are calculated and are represented as Pw,0 and Lw,0. Consequently, it is usual practice to utilise a weight correction approach based on satellite elevations:

$$R = \begin{bmatrix} P_w & & & & \\ & L_w & & & \\ & & \ddots & & \\ & & & P_w & \\ & & & & L_w \end{bmatrix}_{2nX2n} \quad (10)$$

$$P_{w=P_{w,0}} \cdot \frac{1.001}{\sqrt{0.002001 + sin^2(ele)}} \quad (11)$$

$$L_{w=L_{w,0}} \cdot \frac{1.001}{\sqrt{0.002001 + sin^2(ele)}} \quad (12)$$

Then, in order to down-weight the signal affected by scintillation, the code and phase measurements were weighted using MPF and

$$R = \begin{bmatrix} P_{w,scin} & & & & \\ & L_{w,scin} & & & \\ & & \ddots & & \\ & & & P_{w,scin} & \\ & & & & L_{w,scin} \end{bmatrix}_{2nX2n} \quad (13)$$

$$P_{w,scin} = P_w.MPF \;\; or \; P_{w,scin} = P_w.S4 \quad (14)$$

$$L_{w,scin} = L_w.ROTI \;\; or \; L_{w,scin} = L_w\sigma_{\varphi} \quad (15)$$

Where the weights for down-weighting the scintillation impact on code and phase measurements were represented by $P_{w,scin}$ and $L_{w,scin}$, respectively. The primary change in the suggested weight plan is the addition of these two weights. After entering the data into PPPH and weighing the data, the weight strategy followed the same steps as the preceding strategies.

3. Results and Discussion

This section summarizes the results of the Precise Point Positioning (PPP) improvement experiment using 10 days of scintillation-affected data. Section 3.1 presents an instance sample of graphs for visualization, notably from September 13, 2017, at HYD station, due to the significant number of created graphs throughout the 10-day period. In Section 3.2, the complete results for every day are tallied and statistically examined.

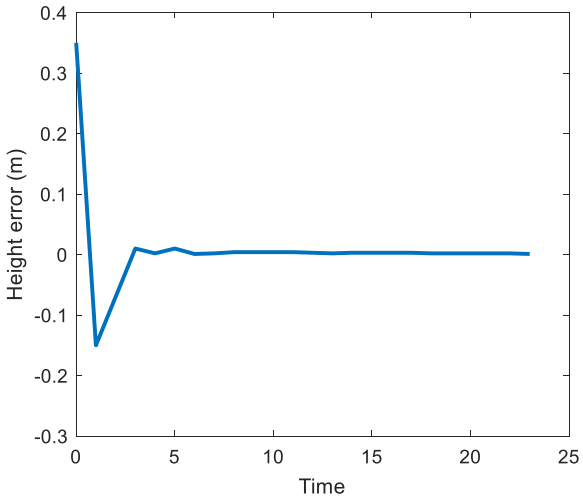

(a)

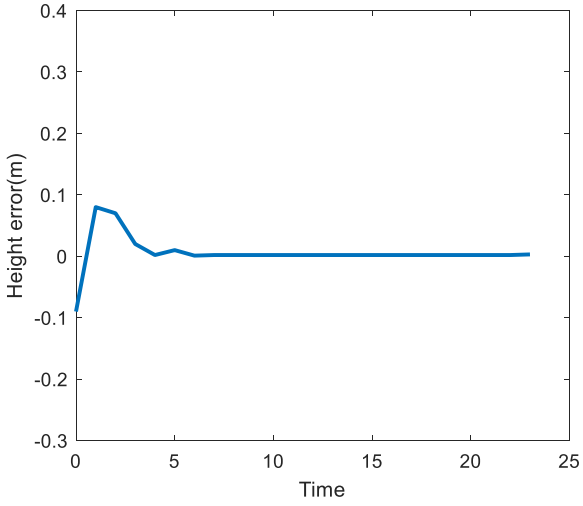

(b)

Figure 3. The height error variation on 1 September 2017 at (**a**) HYD station and (**b**) KNL station.Figure 3. The height error variation on 1 September 2017 at (a) HYD station and (b) KNL station.

Figure 3 shows height error variation at both the stations, HYD and KNL on September 1, 2017. The height estimation acquired a consistent continuous accuracy of around 0.3m and 0.1 m at the convergence time of about 30 min at both the stations. Consequently, the data show that the convergence period of 45 minutes was used for the RMSE computation.

3.1. The Approach of Removing Satellites

Using MP1, MP2, S4 and σ_{φ} as criteria, the satellites most affected by scintillation were found using this method. In particular, I05 was found to be the satellite most impacted by scintillation, although I06 was shown to be more significant on September 13, 2017, at the HYD station, based on the Rate of Change of Total Electron Content Index (ROTI). Based on Root Mean Square Error (RMSE) for the given date, Figure 4 compares the original and I05-removed Precise Point Positioning (PPP) height (a) and 3D error (b).

As can be seen in Figure 4, there is variation in both the starting height and 3D inaccuracies within the first 10 hours. It's interesting to see that after removing I05, the RMSE for height and 3D errors barely changes. This suggests that even though I05 was found to have the highest scintillation based on both scintillation parameters and Multipath Parameters (MP), deleting it did not significantly contribute to error reduction. As a result, the positioning algorithm's overall performance and satellite availability were little affected by the removal of I05.

Moreover, I06 an additional scintillation-affected satellite was eliminated on the basis of ROTI, and a comparable analysis was carried out, as seen in Figure 5. The RMSE in this case showed a minor improvement, with improvement rates of 5.5% and 4.6%, respectively, for both height and 3D errors. The results indicate that during the scintillation phase, eliminating I06 had a somewhat favorable impact.

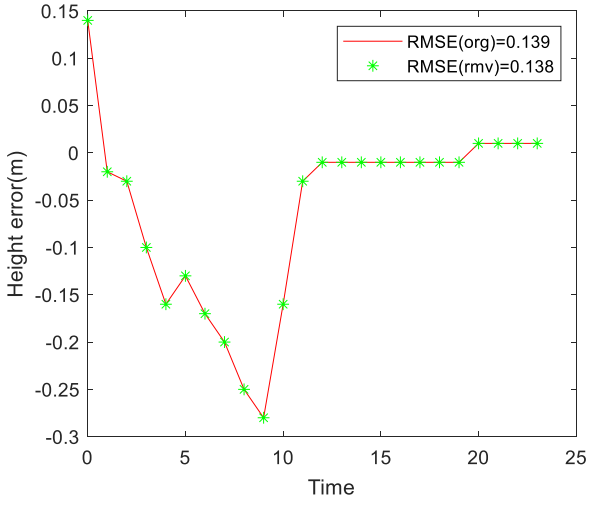

(a)

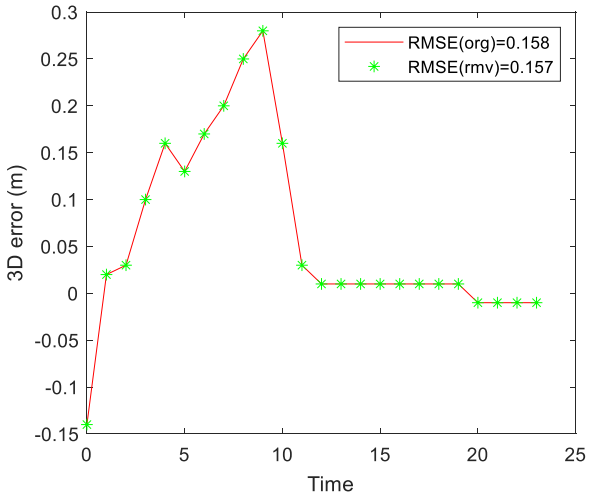

(b)

Figure 4. Comparison between (**a**) the original and I05-removed RMSE of the height error, (**b**) the original and I05-removed RMSE (m) of the 3D error on 13 September 2017 at HYD station.

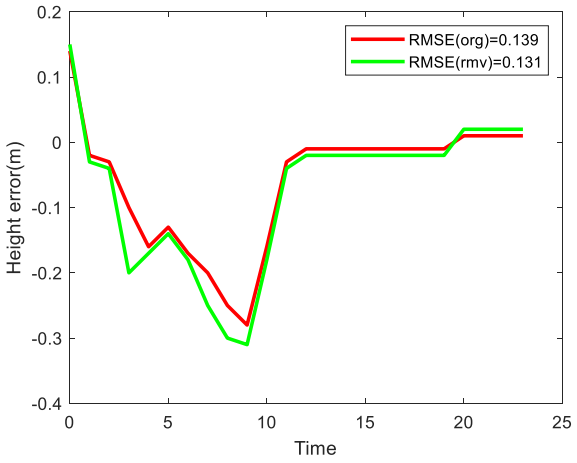

(a)

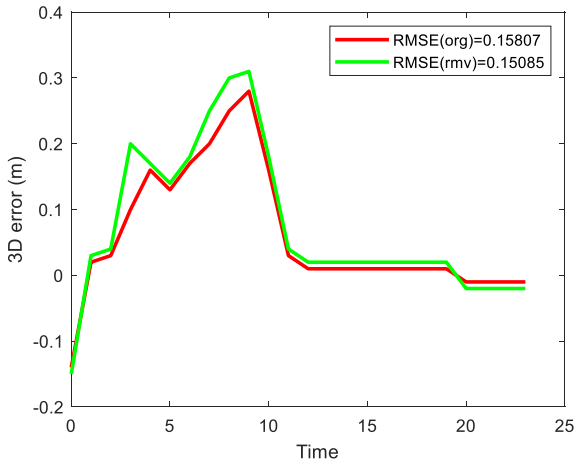

(b)

Figure 5. As Figure 4 except I06 was removed rather than I05.

Geometric Dilution of Precision (GDOP) before and after deleting I05 in order to evaluate the effect of satellite removal on GDOP is analyzed. GDOP levels mostly remain below 5, and all values remain below 8, during the period shown. Interestingly, it is also observed that a little increase in GDOP values throughout the first six hours.

It is noteworthy that six NavIC satellites were accessible throughout the scintillation period. In such cases, the elimination of a single satellite affects satellite geometry and, in turn, Dilution of Precision (DOP) to a limited extent. The hypothesis that the satellite removal method had little effect on DOP during the scintillation period is supported by the continuously low GDOP values, which indicate that the removal of I05 or I06 did not significantly impair the geometric quality of the satellite constellation.

3.2 Observation Removal Approach

The observation removal technique produced more significant improvements in height and 3D errors compared to the satellite removal strategy. These data show that the total deviation from the reference coordinate and the variability during the scintillation affected time were further reduced, and that the most useful threshold was ROTI. Furthermore, the trio of MP1, MP2, and ROTI performed better in lowering 3D error.

After calculating the improvement rates for the findings, the percentages that were obtained were 59.49%, 27.14%, 87.67%, 80.36%, 59.48%, 0.5%, 80.15%, and 81.76%, in that order. Remarkably, the observation removal technique outperformed the satellite removal strategy in terms of improvements, especially when ROTI and MP1, MP2, and ROTI were used together, as improvements above 80.31%. This highlights how well the observation elimination technique works to reduce scintillation impacts on PPP (precise point placement).

Effect of Observation Elimination on GDOP: The GDOP changes brought about by the observation removal method, which focuses on MP1, MP2, ROTI, and their combination. Interestingly, these alterations were noticeably more noticeable than the effects of the satellite removal.

Since ROTI is more sensitive to scintillation than MP, it is noted that ROTI is more likely to exceed the threshold, which leads to the elimination of matching data and greater GDOP values. Furthermore, the combination of MP1, MP2, and ROTI, which is to be expected considering the elimination of a larger amount of data. While both ROTI and the combined method showed greater benefits, the wide range in GDOP may jeopardize the accuracy of the findings. This effect might explain why the combined strategy's height gain was less than that of ROTI alone.

3.3. Increasing Position Accuracy with Weight Strategy:

The weight strategy's results highlight RMSE improvements based on both scintillation and standard parameters. Interestingly, RMSE gains were marginally higher when standard parameters were used instead of scintillation parameters. The improvement rates, which were 71.46%, 72.67%, 73.81%, and 73.14%, respectively.

Although the method of observation elimination showed greater benefits, it also resulted in higher levels of GDOP. Elevated GDOP values indicate near satellite separations and a reduced level of trust in the data obtained from these satellites, which might lead to heightened positional uncertainty. It's important to note that GDOP stayed the same because the weight strategy's implementation had no effect on satellite availability.

3.4. Statistical Analysis of Scintillation Mitigation Strategies

3.4.1. A Comprehensive Analysis of the Satellite Removal Strategy

Tables 1-2 show the outcomes of the satellite removal approach, which was based on a number of criteria over the course of 10 days at two different stations, including MP1, MP2, ROTI, S4, and σ_{φ}. For clarity, improved RMSE values are shown in bold. The results show that the approach for removing satellites, using conventional parameters or scintillation, showed different levels of success.

In particular, the MP1-based approach improved conditions on 7 of the 10 days, whereas the MP2, ROTI, and strategies improved conditions on 8, 6, and 5 days, respectively. Remarkably, only two of the seven days saw an improvement in location errors when using S4, a scintillation parameter. Scintillation parameters were not more effective than conventional parameters overall, with S4 being the least effective of the group.

Furthermore, it was noted that, in some cases, the removal of satellites based on MP improved inaccuracy, but this was not always the case for other parameters, and vice versa. Furthermore, there was inconsistent non-simultaneous improvement in height and 3D inaccuracies. Even while the technique reduced mistakes on up to 8 of the 10 days, these improvements were usually small often less than 0.05 m or even 0.01 m especially in light of the fact that the majority of the initial errors were decimeter-level. As a result, even with different settings, the satellite removal technique did not always work as intended.

Table 1. Change of the height and 3D positioning errors (m) through the satellite removal strategy as represented by the RMSE at HYD.

Station	Date	RMSE(m)		Reference Parameters	Removed Satellite	Satellite Removed RMSE (m)	
		Height	3D			Height	3D
HYD	07-Sep-17	0.15	0.21	MP1	I05	0.0141	0.0168
				MP2			
				ROTI			
				S4			
				Sigma Pi			
	08-Sep-17	0.6245	0.6422	MP1	I05	0.6245	0.6422
				MP2			
				ROTI			
				S4			
				Sigma Pi			
	13-Sep-17	0.1395	0.1581	MP1	I05	0.139	0.1575
				MP2			
				ROTI			
				S4			
				Sigma Pi			

Table 2. Change of the height and 3D positioning errors (m) through the satellite removal strategy as represented by the RMSE at KNL.

Station	Date	RMSE (m)		Reference Parameters	Removed Satellite	Satellite Removed RMSE (m)	
		Height	3D			Height	3D
KNL	04-Sep-17	0.026	0.0345	MP1	I05	0.0304	0.0381
				MP2			
				ROTI			
				S4			
				Sigma Pi			
	07-Sep-17	0.0247	0.0311	MP1	I05	0.029	0.0351
				MP2			
				ROTI			
				S4			
				Sigma Pi			
	08-Sep-17	0.1355	0.3454	MP1	I05	0.1353	0.3456
				MP2			
				ROTI			
				S4			
				Sigma Pi			
	13-Sep-17	0.0219	0.0329	MP1	I05	0.0221	0.0331
				MP2			
				ROTI			
				S4			
				Sigma Pi			

3.4.2. Observation Removal Approach

Table 3 presents a detailed analysis of the improvement in height and 3D positioning errors after scintillation-affected observations were removed using both Mild Threshold (MT) and Extreme Threshold (ET) criteria. This analysis takes into account permutations and combinations of MP1, MP2, ROTI, S4, and σ_{φ} over a 10-day period at 2 stations. A summary is given in the main paper, however in the supplemental material show more comprehensive data due to the large number of combinations.

Two primary metrics are used to evaluate this strategy: the percentage of days with improvement and the greatest rate of progress. Only seven days were spent using S4 at two sites (not SNA0P, where S4 values were poor). The height and 3D errors improved on 8/10 day, when S4 was excluded from comparison. The most notable improvement rates were 91.37%, attained using standard parameters. It is worth noting that the maximum percentage of days (8/10) exhibiting reductions in height errors were noted while using both standard and scintillation parameters. In contrast, the introduction of scintillation characteristics resulted in the biggest number of days with improvement for 3D errors. This implies that standard parameters often provide a more noticeable level of enhancement, whereas scintillation parameters are more likely to cause improvement.

The probability and degree of improvement were comparatively low whether MP1 and MP2 were used alone or in tandem. For instance, using MP2 by itself in conjunction with the ET criteria produced results that were significantly lower than other scenarios, with the greatest improvement rate in height errors being 16.23% and the proportion of days with improvement being 3/10. On the other hand, when MP and ROTI were used together, the improvement was on par with or even greater than when ROTI was used alone. Notably, the combination of MP1 and ROTI demonstrated a better likelihood and amount of improvement compared to other combinations of standard parameters.

Additionally, when comparing the effectiveness of Mild Threshold (MT) with Extreme Threshold (ET), MT typically showed better results in terms of the greatest improvement rate and the percentage of days with improvement. For the best improvement rate, the proportion of days with improved 3D mistakes consistently outpaced that of height errors.

Additionally, the efficacy of scintillation parameters and ROTI was equivalent when a single reference parameter was used. Nevertheless, out of all the combinations, MP1 and ROTI proved to be the most reliable combination, showing a higher chance and degree of improvement. This implies that, in comparison to individual factors, the combination of MP and ROTI might successfully offset a wider spectrum of errors.

3.4.3. Weight Strategy

The improvements in height and 3D errors made possible by the weight approach throughout a 10-day period at two sites. For clarity, improved Root Mean Square Errors (RMSEs) are indicated in bold. The height RMSE was improved by scintillation and standard parameters separately on 6 and 8 of the 10 days, with the greatest improvement rates being 93.14% and 86.15%, respectively. Scintillation and standard parameters improved 3D RMSE on 8 and 7 of the 10 days, respectively, for 3D errors. The greatest improvement rates were 85.52% and 73.44%, respectively. Based on the percentage of days with improvement and the greatest improvement rate, it can be observed that standard parameters within the weight strategy were similar to scintillation parameters in terms of improving both height and 3D errors. Furthermore, there was a continuous greater improvement in height error than in 3D error.

4. Discussion

The position improvement trials made use of data from two stations (HYD and KNL) that covered a period of 70 days. These studies focused on 10 days with scintillation and employed three mitigation measures to improve location accuracy. In Section 3.1, we evaluated the PPPH convergence time between the two stations and found that, on days without scintillation, it was around half an hour (Figure 3). After that, an example of a visualization based on data from September 13, 2017, at HYD was given.

Based on many criteria, satellites I05 and I06 were determined to be undergoing the strongest scintillation in the first strategy. On the other hand, eliminating I06 led to only moderate gains (5.5% in height and 4.6% in 3D error), while eliminating I05 had no effect on RMSE for either height or 3D errors. When compared to previous tactics, this one proved to be less successful, which raised concerns regarding the characteristics of the deleted satellites and other circumstances that would result in PPP enhancements. Furthermore, the loss of a single satellite had no impact on GDOP when the number of satellites was high and the geometry was appropriate.

The observation removal technique produced more significant gains. Compared to MP1 and MP2, ROTI-based criteria produced better improvement rates above 80%. Combining variables like MP1, MP2, and ROTI produced notable improvements that had improvement rates of more than 80%. Using MT (multipath threshold), in particular, the observation removal technique performed better than the satellite removal strategy. Care must be used though, as selecting a bigger MT might affect the geometry of the satellite and raise GDOP, which would affect positional stability.

A steady substitute was offered by the weight approach, which was covered in Section 3.1.4 and showed improvements without impacting GDOP. Comparable gains were seen between scintillation and standard values. The weight technique provided steady, dependable gains, although it was not as effective as the observation removal strategy.

The satellite removal technique was less successful, resulting in improvements on just a few days and frequently of little importance, according to Tables 1-2, which summarise data over a 10-day period. On the other hand, the approach of observation elimination shown more significant advancements, with promising scintillation parameters. Even while the weight method showed a smaller percentage of improved days, on other days it showed greater benefits. In summary, the selection of a mitigation method is contingent upon particular circumstances, with the technique of observation elimination providing notable enhancements. On the other hand, the weight technique offers consistent and dependable gains without affecting the geometry or availability of satellites. The study emphasizes that for PPP improvement to be effective, cycle slip events, elevation angles, and satellites influenced by scintillation must all be carefully taken into account.

Moreover, there may be situations when one works when the other does not, and vice versa, due to differences in the effectiveness of standard and scintillation parameters. Standard parameters, in particular MP, are able to describe scintillation and multipath effects, which may make them more adaptable for down-weighting different kinds of errors. This adaptability raises the possibility that conventional settings might mitigate scintillation effectively. On the other hand, because they may more accurately capture scintillation, scintillation parameters such as ROTI may perform better in situations where conventional parameters are inadequate.

Crucially, our approach removed the rigid reliance on scintillation parameters and provided an alternative with equal performance utilizing standard parameters (MP and ROTI). This adaptability makes it possible to use data with a 1-second time interval, which enhances the scope of the scintillation investigation. The reach and breadth of scintillation studies are increased by utilizing data from NavIC.

To further increase location accuracy, future research may examine the integration of data from many other GNSS constellations. In particular, a fruitful direction might be to assess the weight and observation removal procedures with an emphasis on satellite geometry. Because the observation removal technique benefits from more visible satellites, it may be able to retain superior satellite geometry when applied to several GNSS. Furthermore, the implementation of sophisticated techniques like genetic algorithms, machine learning, and Bayesian optimization may improve the effectiveness and uniformity of the weight scheme. Therefore, more investigation is necessary to evaluate these techniques' effectiveness utilizing these cutting-edge methodologies.

5. Conclusion

In order to reduce scintillation effects on Precise Point Positioning (PPP), this study investigated three different approaches: satellite removal, observation removal, and a unique weighting strategy.

Every method demonstrated distinct features and results, offering important new perspectives on scintillation reduction. The small amount of increase in location accuracy was obtained using the satellite removal approach. On the other hand, the approach of observation removal constantly showed significant improvements, demonstrating its efficacy. The strategy's dependence on deleting observations may lead to instability, mostly because of changes in GDOP brought about by large deletions. One possible way to overcome this constraint is to investigate data from several satellite constellations. The most promising method was the weight technique, which produced surprisingly 93.14% improvement in height inaccuracy. Notably, in both the weight and observation removal procedures, conventional metrics like MP and ROTI demonstrated performance parity with scintillation parameters. The observation removal approach is a noteworthy invention, even with its recognized drawbacks. Notwithstanding its drawbacks, this approach offers a convenient substitute for the weight technique while yielding steady improvements in error rates.

References

[1] Aquino, M.; Sreeja, V. Correlation of scintillation occurrence with interplanetary magnetic field reversals and impact on Global Navigation Satellite System receiver tracking performance. Space Weather 2013, 11, 219–224.

[2] Li, Q.; Su, X.; Xu, Y.; Ma, H.; Liu, Z.; Cui, J.; Geng, T. Performance Analysis of GPS/BDS Broadcast Ionospheric Models in Standard Point Positioning during 2021 Strong Geomagnetic Storms. Remote Sens. 2022, 14, 4424.

[3] Luo, X.; Liu, Z.; Lou, Y.; Gu, S.; Chen, B. A study of multi-GNSS ionospheric scintillation and cycle-slip over Hong Kong region for moderate solar flux conditions. Adv. Space Res. 2017, 60, 1039–1053.

[4] Humphreys, T.E.; Psiaki, M.L.; Kintner, P.M. Modeling the effects of ionospheric scintillation on GPS carrier phase tracking. IEEE Trans. Aerosp. Electron. Syst. 2010, 46, 1624–1637.

[5] Van Dierendonck, A.J.; Klobuchar, J.A.; Hua, Q. Ionospheric Scintillation Monitoring Using Commercial Single Frequency C/A Code Receivers. In Proceedings of the 6th International Technical Meeting of the Satellite Division of the Institute of Navigation, Salt Lake City, UT, USA, 22–24 September 1993.

[6] Aquino, M.; Dodson, A.; deFranceschi, G.; Alfonsi, L.; Romano, V.; Monico, J.; Marques, H.; Mitchell, C. Towards forecasting and mitigating ionospheric scintillation effects on GNSS. In Proceedings of the ELMAR 2007, Zadar, Croatia, 12–14 September 2007.

[7] Conker, R.S.; El-Arini, M.B.; Hegarty, C.J.; Hsiao, T. Modeling the effects of ionospheric scintillation on GPS/Satellite-Based Augmentation System availability. Radio Sci. 2003, 38, 1001.

[8] Aquino, M.; Monico, J.F.G.; Dodson, A.H.; Marques, H.; De Franceschi, G.; Alfonsi, L.; Romano, V.; Andreotti, M. Improving the GNSS positioning stochastic model in the presence of ionospheric scintillation. J. Geod. 2009, 83, 953–966.

[9] Park, J.; Vadakke Veettil, S.; Aquino, M.; Yang, L.; Cesaroni, C. Mitigation of Ionospheric Effects on GNSS Positioning at Low Latitudes. Navigation 2017, 64, 67–74.

[10] Vadakke Veettil, S.; Aquino, M.; Marques, H.A.; Moraes, A. Mitigation of ionospheric scintillation effects on GNSS precise point positioning (PPP) at low latitudes. J. Geod. 2020, 94, 15.

[11] de Oliveira Moraes, A.; Costa, E.; de Paula, E.R.; Perrella, W.J.; Monico, J.F.G. Extended ionospheric amplitude scintillation model for GPS receivers. Radio Sci. 2014, 49, 315–329.

[12] Bougard, B.; Simsky, A.; Sleewaegen, J.-M.; Park, J.; Aquino, M.; Spogli, L.; Romano, V.; Mendonça, M.; Monico, G. CALIBRA: Mitigating the impact of ionospheric scintillation on Precise Point Positioning in Brazil. In Proceedings of the GNSS Vulnerabilities and Solutions Conference, Baška, Krk Island, Croatia, 18–20 April 2013.

[13] Marques, H.A.; Marques, H.A.S.; Aquino, M.; Vadakke Veettil, S.; Monico, J.F.G. Accuracy assessment of Precise Point Positioning with multi-constellation GNSS data under ionospheric scintillation effects. J. Space Weather Space Clim. 2018, 8, A15.

[14] Vilà-Valls, J.; Linty, N.; Closas, P.; Dovis, F.; Curran, J.T. Survey on signal processing for GNSS under ionospheric scintillation: Detection, monitoring, and mitigation. Navigation 2020, 67, 511–536.

[15] Nguyen, V.K.; Rovira-Garcia, A.; Juan, J.M.; Sanz, J.; González-Casado, G.; La, T.V.; Ta, T.H. Measuring phase scintillation at different frequencies with conventional GNSS receivers operating at 1 Hz. J. Geod. 2019, 93, 1985–2001.

[16] Luo, X.; Gu, S.; Lou, Y.; Cai, L.; Liu, Z. Amplitude scintillation index derived from C/N0 measurements released by common geodetic GNSS receivers operating at 1 Hz. J. Geod. 2020, 94, 27.

[17] Zhao, D.; Li, W.; Li, C.; Tang, X.; Zhang, K. Extracting an ionospheric phase scintillation index based on 1 Hz GNSS observations and its verification in the Arctic region. Acta Geod. Et Cartogr. Sin. 2021, 50, 368–383.

[18] Zhao, D.; Li, W.; Li, C.; Tang, X.; Wang, Q.; Hancock, C.M.; Roberts, G.W.; Zhang, K. Ionospheric Phase Scintillation Index Estimation Based on 1 Hz Geodetic GNSS Receiver Measurements by Using Continuous Wavelet Transform. Space Weather 2022, 20, e2021SW003015.

[19] IGS. International GNSS Service. Available online: https://igs.org/ (accessed on 23 November 2021).

[20] Li, C.; Hancock, C.M.; Hamm, N.A.S.; Vadakke Veettil, S.; You, C. Analysis of the Relationship between Scintillation Parameters, Multipath and ROTI. Sensors 2020, 20, 2877.

[21] Yang, Z.; Liu, Z. Correlation between ROTI and Ionospheric Scintillation Indices using Hong Kong low-latitude GPS data. GPS Solut. 2016, 20, 815–824.

[22] Olwendo, J.O.; Cilliers, P.; Weimin, Z.; Ming, O.; Yu, X. Validation of ROTI for Ionospheric Amplitude Scintillation Measurements in a Low-Latitude Region Over Africa. Radio Sci. 2018, 53, 876–887.

[23] Acharya, R.; Majumdar, S. Statistical relation of scintillation index S4 with ionospheric irregularity index ROTI over Indian equatorial region. Adv. Space Res. 2019, 64, 1019–1033.

[24] Basu, S.; Groves, K.M.; Quinn, J.M.; Doherty, P. A comparison of TEC fluctuations and scintillations at Ascension Island. J. Atmos. Sol.-Terr. Phys. 1999, 61, 1219–1226.

[25] Romano, V.; Spogli, L.; Aquino, M.; Dodson, A.; Hancock, C.; Forte, B. GNSS station characterisation for ionospheric scintillation applications. Adv. Space Res. 2013, 52, 1237–1246.

[26] Hancock, C.M.; Ligt, H.D.; Xu, T. The possibility of using GNSS quality control parameters to assess ionospheric scintillation errors. In Proceedings of the Fig WorkingWeek, Helsinki, Finland, 29 May–2 June 2017.

[27] Li, C.; Hancock, C.M.; Vadakke Veettil, S.; Zhao, D.; Galera Monico, J.F.; Hamm, N.A.S. Distinguishing ionospheric scintillation from multipath in GNSS signals using geodetic receivers. GPS Solut. 2022, 26, 150.

[28] Bahadur, B.; Nohutcu, M. PPPH: A MATLAB-based software for multi-GNSS precise point positioning analysis. GPS Solut. 2018, 22, 113.

[29] Pi, X.; Mannucci, A.J.; Lindqwister, U.J.; Ho, C.M. Monitoring of global ionospheric irregularities using the Worldwide GPS Network. Geophys. Res. Lett. 1997, 24, 2283–2286.

[30] Estey, L.H.; Meertens, C.M. TEQC: The Multi-Purpose Toolkit for GPS/GLONASS Data. GPS Solut. 1999, 3, 42–49.

[31] Estey, L.; Meertens, C. Teqc Tutorial: Basic of Teqc Use and Teqc Products; UNAVCO Inc.: Boulder, CO, USA, 2014.

[32] Axelrad, P.; Brown, R.G. GPS Navigation Algorithms. In Global Positioning System: Theory and Applications, Volume I; American Institute of Aeronautics and Astronautics: Reston, VA, USA, 1996; pp. 409–433.

[33] An, X.; Meng, X.; Jiang, W. Multi-constellation GNSS precise point positioning with multi-frequency raw observations and dual-frequency observations of ionospheric-free linear combination. Satell. Navig. 2020, 1, 7.

[34] Jiao, Y.; Morton, Y.T. Comparison of the effect of high-latitude and equatorial ionospheric scintillation on GPS signals during the maximum of solar cycle 24. Radio Sci. 2015, 50, 886–903.

[35] Mireault, Y.; Tétreault, P.; Lahaye, F.; Héroux, P.; Kouba, J. Online precise point positioning: A new, timely service from Natural Resources Canada. GPS World 2008, 19, 59–64.

[36] Spilker, J. Satellite Constellation and Geometric Dilution of Precision. In Global Positioning System: Theory and Applications, Volume I; American Institute of Aeronautics and Astronautics: Reston, VA, USA, 1996; pp. 177–208.

[37] Lulu, W.; Zaimin, H.; Zhenxing, H.; Yuanyuan, H.; Gang, L. Single-chain hyperbolic positioning GDOP calculation based on longitude transformation method. J. Time Freq. 2020, 43, 196–203.

[38] Mohammed, J.J. Precise Point Positioning (PPP): GPS vs. GLONASS and GPS+GLONASS with an Alternative Strategy for Tropospheric Zenith Total Delay (ZTD) Estimation. Ph.D. Thesis, University of Nottingham, Nottingham, UK, 2017. Unpublished work.

[39] K.C.T.Swamy, Devanaboyina, Venkata Ratnam, Nallagarla, Ramamurthy, Shaik, Towseef Ahmed and Turpati, Suman. "Correlation between rate of TEC index and positioning error during solar flares and geomagnetic storms using navigation with Indian constellation receiver measurements" *Journal of Applied Geodesy*, 2024.

[40] Roberts, G.W.; Fossá, S.; Jepsen, C. Temporal characteristics of triple-frequency GNSS scintillation during a visible aurora borealis event over the Faroe Islands amid a period of very low solar activity. GPS Solut. 2019, 23, 89.

[41] Zhang, X.; Li, P.; Tu, R.; Lu, X.; Ge, M.; Schuh, H. Automatic Calibration of Process Noise Matrix and Measurement Noise Covariance for Multi-GNSS Precise Point Positioning. Mathematics 2020, 8, 502.

[42] Langley, R.B. Dilution of Precision. In GPS World; North Coast Media: Cleveland, OH, USA, 1999; Volume 10, pp. 52–59.

[43] Guo, F.; Zhang, X. Adaptive robust Kalman filtering for precise point positioning. Meas. Sci. Technol. 2014, 25, 105011.

[44] K.C.T. Swamy, D. Venkata Ratnam, T. Suman, S. Towseef Ahmed, Time-differenced double difference method for measurement of Navigation with Indian Constellation (NavIC) receiver differential phase bias,
Measurement, Volume 207, 2023, 112385.